Magnetic Resonance Imaging with Respiratory Gating: Techniques and Advantages

Richard L. Ehman[1]
Michael T. McNamara[1]
Michael Pallack[2]
Hedvig Hricak[1]
Charles B. Higgins[1]

Respiratory motion is an important problem in magnetic resonance imaging (MRI) of the thorax and upper abdomen. This study assessed several approaches for practical respiratory gating. Methods of acquiring respiratory signals, gated sequencing methods, duration of examination, strategies for reducing examination time, diagnostic quality of gated images, and the influence of respiratory gating on relaxation time measurements were evaluated. Of three different devices for acquiring the respiratory signal, a belt containing a displacement transducer placed around the upper abdomen was found to be most effective and practical. Two pulse-gating modes were implemented, as well as a method for combining cardiac and respiratory gating. Gating methods were tested using phantoms and human volunteers.

A spin-conditioned mode of respiratory gating was found to be superior to a more simply implemented triggered mode in which spin-echo (SE) sequencing was interrupted. The time penalty for respiratory gating is technique-dependent. Gated studies with uncontrolled tidal breathing took two to four times longer than nongated studies. When the time between respirations was voluntarily prolonged, gated studies could be only 30%–50% longer than nongated. The standard deviation of relaxation-time measurements for organs that are displaced during respirations was substantially reduced by respiratory gating. Gating acquisition without spin-conditioning caused systematic errors in T1 relaxation times that were not present with spin-conditioned gating. Respiratory gating is a practical and useful technique for improving the contrast and spatial resolution of SE images of the upper abdomen and chest. SE images produced with short repetition times were particularly improved by respiratory gating.

The time required for acquisition of magnetic resonance (MR) images with high spatial and contrast resolution is long in comparison with the time scale of physiologic motions, such as cardiac contraction with the time scale of physiologic motions, such as cardiac contraction, respiratory motion, and even gastrointestinal peristalsis. Even though multislice and multiecho acquisition techniques improve clinical throughput, these do not reduce the total time of data collection for the individual anatomic sections [1, 2]. Physiologic motion still degrades the images by causing a variety of artifacts [3–5]. One of the major obstacles to further improvement of the diagnostic quality of MR images of the chest and upper abdomen is respiratory motion. Gated data acquisition has been used with great success for imaging the heart [6, 7]. Similarly gated acquisition techniques have been demonstrated for reduction of the effect of respiratory motion on MR images [8, 9].

However, questions remain regarding the ideal technique for acquiring the respiratory pulse, the method for synchronizing radiofrequency pulses to the respiratory cycle, and the possible effect of respiratory gating on the relaxation times calculated from MR images.

We evaluated several methods for obtaining respiratory signals suitable for use in respiratory gating, determined the best time in the respiratory cycle for data acquisition, and evaluated different approaches to regulating imager sequencing and data collection. In addition, the effect of respiratory gating on measurement of

Received July 2, 1984; accepted after revision September 5, 1984.

[1] Department of Radiology, University of California School of Medicine, San Francisco, CA 94143. Address reprint requests to C. B. Higgins.

[2] Diasonics, MRI Division, South San Francisco, CA 94080.

AJR 143:1175–1182, December 1984
0361–803X/84/1436–1175

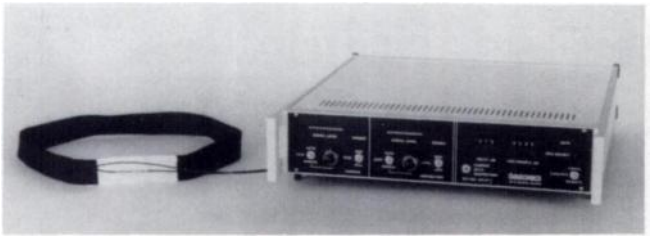

Fig. 1.—Device for acquiring respiratory signal (*left*). Belt is placed around upper abdomen. Fiberoptic system senses stretching of short elastic segment of belt and transmits information to gating control unit (*right*).

relaxation times was assessed, and the types of spin-echo (SE) sequences that were most improved by respiratory gating were determined.

Subjects and Methods

Respiratory Signal Acquisition

Three different devices were constructed for acquiring a respiratory signal. The first was based on a small plastic mask of the type used for oxygen therapy, fitting over the nose and mouth. A thermistor was mounted in the orifice of the mask for sensing the temperature of respiratory air. A respiratory signal was obtained by monitoring the temperature sensor; expired air is warmer than inspired air. The electrical signal from the sensor was converted to an optical signal by a small battery-powered interface unit attached to the patient. The optical signal was transmitted out of the bore of the magnet via a fiberoptic cable to a receiver interface and gating control electronics.

A second respiratory monitor was constructed by fitting a small thermal sensor to nose tip of a nasal-cannula-type oxygen administration device. The monitor worked on the same principle as the first device, sensing temperature changes in air passing through the nares. The same interface equipment was used.

The third device consisted of a belt circling the upper abdomen. Changes in the length of a short elastic segment during breathing were sensed by a simple passive light-modulation device (fig. 1). The optical signal was transmitted by a fiberoptic cable directly from the belt to the receiver interface.

The receiver interface converted the optical signals; after baseline correction and signal conditioning, the respiratory signal was displayed on a cathode ray tube (CRT) and a strip chart recorder (fig. 2). Control electronics allowed generation of an enable signal for data acquisition in any segment of the respiratory cycle.

Modes of Respiratory Gating

Two modes of respiratory gating were implemented by making appropriate hardware and software modifications to the sequence control computer and data handling electronics of the imager. The first was a triggered (non-spin-conditioned) mode in whch SE sequencing at the predetermined repetition time (TR) is turned on and off at appropriate times in the respiratory cycle under control of the enabling signal from the gating control box (fig. 3). In this mode, tissues are subject to long periods of relaxation when radiofrequency irradiation is switched off by the gating system in response to respiratory motion.

The second (spin-conditoned) mode required more hardware and software changes than the non-spin-conditioned gating mode. In this approach, SE sequencing runs continuously at a preset TR. The

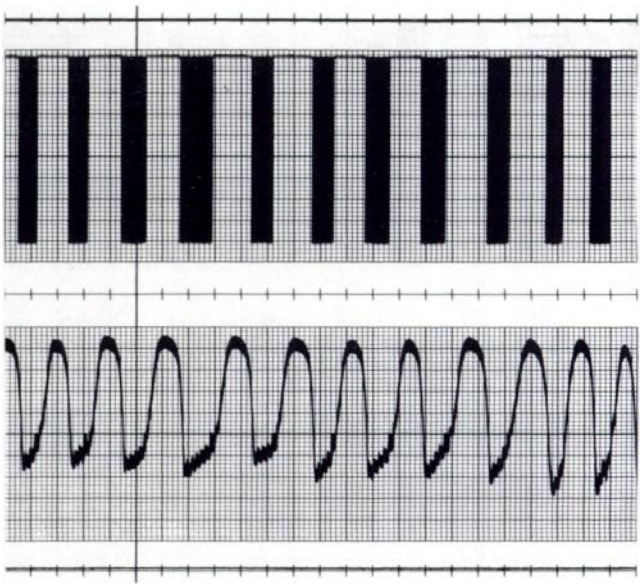

Fig. 2.—Respiratory signal for tidal breathing (*lower trace*). Upgoing curve indicates inspiration. *Vertical bars* above respiratory trace indicate when imager is acquiring data.

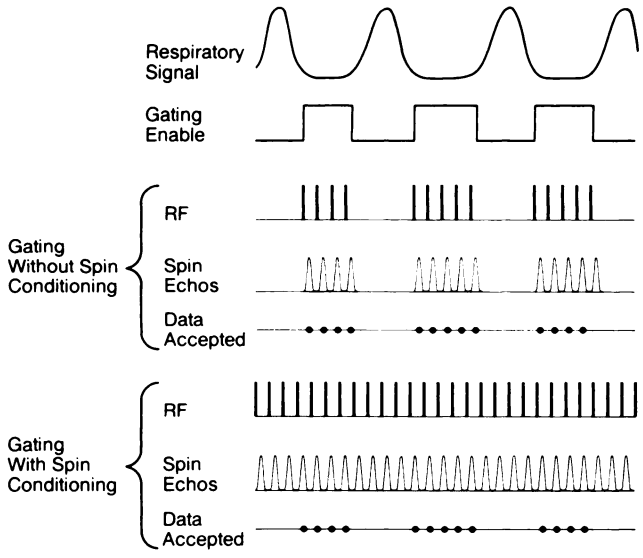

Fig. 3.—Comparison of respiratory gating with and without spin-conditioning. Note that in mode without spin-conditioning, radiofrequency (RF) irradiation is periodically interrupted for periods that are longer than normal repetition time.

enabling signal from the gating system is used to determine which spin echoes from the incoming stream will be kept by the computer for image reconstruction (fig. 3). When enough echoes have been collected at a given phase encoding setting, the system is allowed to go on to the next setting. Thus, tissue is not allowed to relax for long periods of time when data cannot be collected.

A method for combined cardiac and respiratory gating was tested. In this technique, cardiac-gated acqusition takes place only at appropriate times in the respiratory cycle, as set by the controls of the gating system.

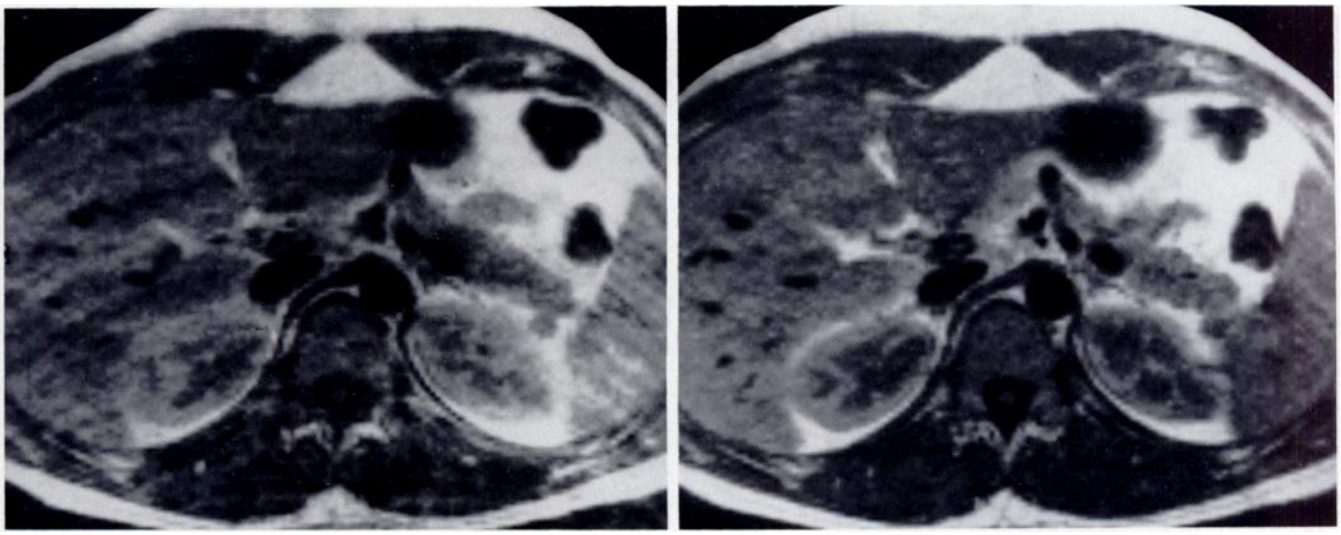

A B

Fig. 4.—Nongated (**A**) and gated (spin-conditioned) (**B**) SE 500/28 images at same anatomic level. General reduction of artifacts and improved depiction of internal renal anatomy in gated study.

Imaging

Examinations were performed on an MR imager (Diasonics MT/S) using a 0.35-T superconducting magnet for proton imaging at 15 MHz [2]. All respiratory and cardiorespiratory gating was performed with multisection imaging, with acquisition of five to 20 sections simultaneously, depending on the TR. A modified Carr-Purcell, dual-spin-echo sequence was used routinely, with echo times (TE) of 28 and 56 msec. The image used 128 × 256 pixels; the voxel dimensions were 7 × 2 × 2 mm.

Subjects

Ten volunteers were imaged in these studies. The volunteers were physicians familiar with the MR imaging procedure. In five volunteers, nongated studies were compared with spin-conditioned respiratory-gated studies at the same anatomic levels. Spin-conditioned images were also compared with corresponding non-spin-conditioned studies in two of these subjects. Transaxial imaging was performed, with the image volume centered at the level of the pancreas. Multisection imaging was performed with two different TRs in all cases so that relaxation times could be calculated. Combined cardiorespiratory gating was performed in three subjects. Transaxial imaging was performed at the level of the heart. Two of the volunteers had imaging in the sagittal and/or coronal planes in the thorax.

In order to more accurately determine the possible effects of the two different modes of gating on relaxation times, a series of experiments with phantoms was conducted. A 12-cm-diam cylindrical phantom was constructed and filled with a doped gelatin material with relaxation times (T1 = 430 msec, T2 = 58 msec) similar to those of many abdominal tissues. The stationary phantom was first imaged using conventional sequences with 500 and 2000 msec TR. It was then imaged with both modes of gating driven by a pulse generator simulating a respiratory rate of 15/min. Relaxation times were calculated in human and phantom images using mean intensities from regions of interest containing at least 100 pixels and a dual-spin-echo model [10, 11].

Results

Gating Methods

All three devices provided respiratory signals that were suitable for controlling the imager. However, when the two airway-temperature devices were used for extended periods, problems became apparent. The mask required good seal with the face in order to obtain a satisfactory signal. As a result, the volunteers reported it was excessively uncomfortable when worn for extended periods. In addition, it contributed to a claustrophobic sensation within the imager.

The thermal sensor mounted on "nasal" prongs was more comfortable for extended wear and did not contribute to claustrophobic sensations. Unfortunately, slight changes in position of the nasal thermistor and variations in nasal airflow caused fluctuation of the signal amplitude during extended imaging. This led to inconsistent acquisition of image data.

The belt device was found to be most satisfactory by all criteria. Once it was positioned and adjusted at the beginning of the study, volunteers were essentially unaware of its presence. The respiratory signal was relatively free from drift. A number of positions in the thorax and abdomen were tested. The most consistent results were obtained by placing the belt just caudad from the anterior costal margin in the upper abdomen.

Effect on Image Quality

Figures 4 and 5 show nongated and corresponding gated (spin-conditioned) studies in which data acquisition took place between end-expiration and the beginning of inspiration. Marked improvement in the diagnostic quality of the gated images was apparent. TR for figures 4, 5A, and 5B was 500

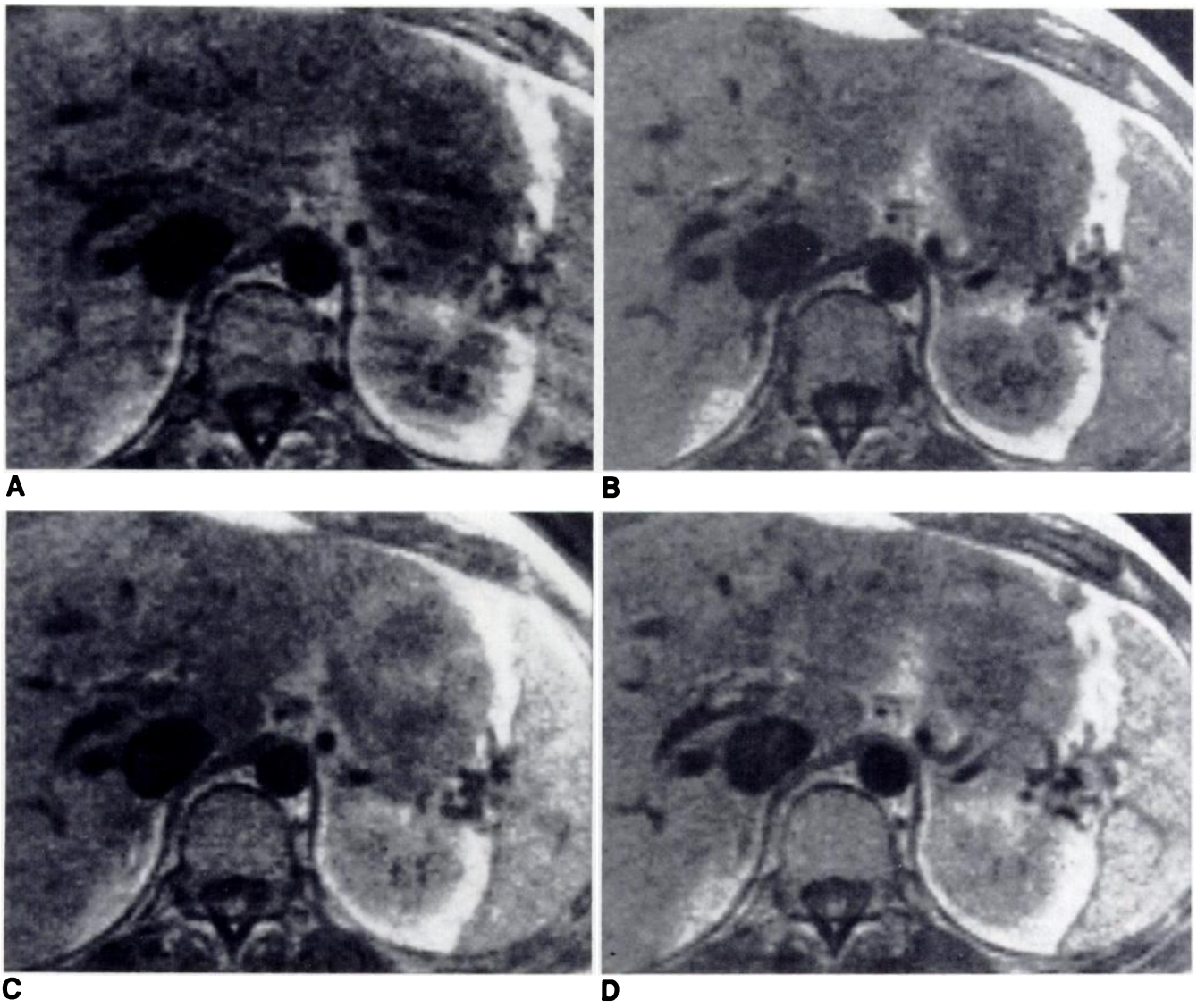

Fig. 5.—Nongated (**A**) and gated (spin-conditioned) (**B**) SE 500/28 images. Nongated (**C**) and gated (spin-conditioned) (**D**) SE 1000/28 images at same level. Superimposed ghost artifacts in nongated images (**A** and **C**) are more apparent than in corresponding gated images (**B** and **D**). Improvement is greater at short TR. Note improved sharpness of vessels in liver and splenic hilum.

msec. We have observed that respiratory-motion artifact in the form of superimposed ghost images is most pronounced in nongated images acquired with short TRs. It is these images that show the greatest improvement with respiratory gating. The differentiation of renal cortex from medulla was notably improved (figs. 4B and 5B).

Images of structures displaced during respiration are subject to blurring even in the absence of a short artifact. This is not apparent in small, high-contrast structures, such as blood vessels. The effect of reducing motion blur by respiratory gating is particularly well demonstrated by comparing the appearance of splenic hilar vessels as shown in figures 5A and 5B.

Figures 5C and 5D are nongated and gated images at the same anatomic levels as figures 5A and 5B but with twice the repetition time (1000 msec TR). They demonstrate that the improvement with respiratory gating at a longer TR is mainly due to reduction of motion blur, since ghost artifacts are not as prevalent at this repetition time.

Several different segments of the respiratory cycle were evaluated from image data acquisition. The segment that provided the greatest reduction of artifact was from end-expiration to the beginning of inspiration.

When nongated imaging was immediately followed by gated imaging at the same anatomic level, we noted that corresponding sections did not match exactly. This effect was

due to the fact that the liver, spleen, and other mobile organs were located at a more cephalad level, on average, in the gated image acquired at end-expiration.

Duration of Gate Imaging

The length of time needed to acquire respiratory-gated images varied widely. In tidal breathing, the length and flatness of the respiratory pause after end-expiration varied from subject to subject depending on respiratory rate, depth, and peak flow rates. The time penalty for respiratory gating with spontaneous tidal breathing depended on the pattern of breathing and the threshold value that was considered to represent end-expiration. Respiratory gating with tidal breathing required two to four times more scanning time than nongated studies when TR was 500 msec. The time penalty was proportionately less for studies with longer TRs. For example, it averaged about twice as long with 1000 msec TR.

Scanning time with respiratory gating was drastically reduced by instituting a prescribed pattern of breathing. Volunteers simply were instructed to lengthen the time between breaths (fig. 6). Imaging time was reduced to only 30%–50% longer than nongated studies without compromising the quality of the images.

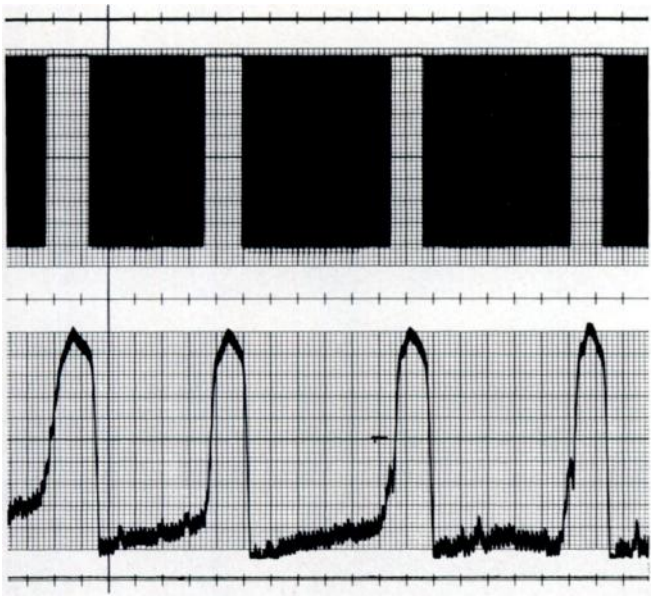

Fig. 6.—Respiratory signal (*lower trace*) from volunteer instructed to lengthen time between breaths. Note increased tidal volume compared with normal breathing in fig. 2. *Dark bars* indicate when imager is acquiring data. Proportion of imaging time lost due to breathing is less than in fig. 2.

Influence of Spin-Conditioning

Comparison of images obtained with the spin-conditioned mode of respiratory gating and the non-spin-conditioned mode demonstrated that more ghost artifacts were present in the non-spin-conditioned images, especially at short TRs. With long TRs, differences were less apparent, except at the level of the diaphragm, where ghosting was a particular problem (fig. 7). No significant differences in imaging times were observed with the two modes.

Combined Cardiac and Respiratory Gating

Combined gating resulted in images that showed slightly more internal cardiac detail than with cardiac gating alone (fig. 8). Combined cardiorespiratory gating in the coronal plane showed slightly improved definition of the domes of the diaphragm (fig. 9), but little improvement in depiction of cardiac anatomy compared with cardiac gating alone. The time penalty for combined gating was the same as for respiratory-gated studies with TRs equivalent to the cardiac period.

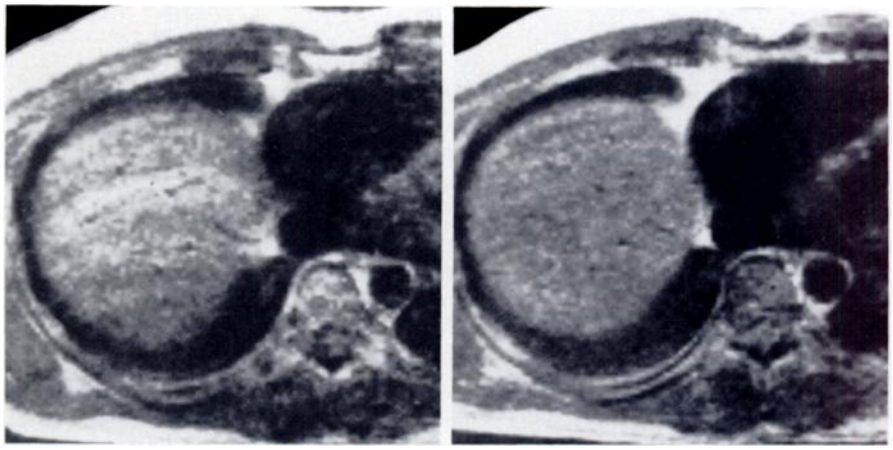

Fig. 7.—Comparison of respiratory gating without (**A**) and with (**B**) spin-conditioning. Note reduction of artifact in dome of liver with spin-conditioning.

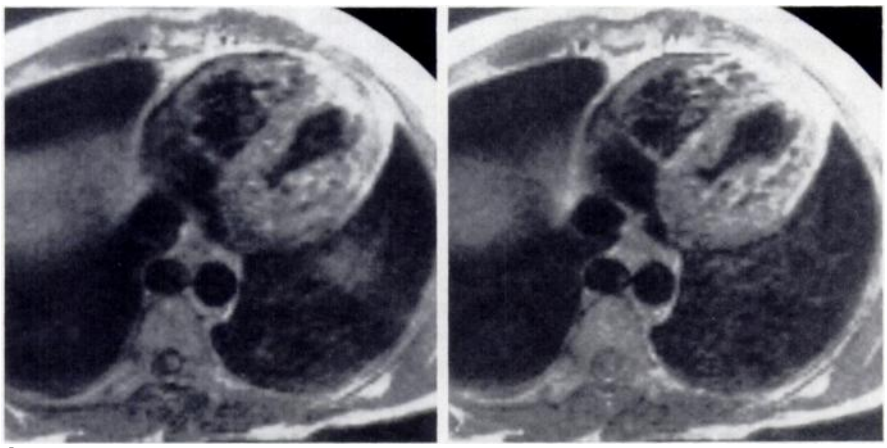

Fig. 8.—Cardiac gating (**A**) and combined cardiac and respiratory gating (**B**). Details of cardiac anatomy, such as trabeculation in right ventricle, are slightly sharper with combined gating (**B**). Note enlarged azygos vein adjacent to aorta in this subject with azygos continuation of interrupted suprarenal vena cava.

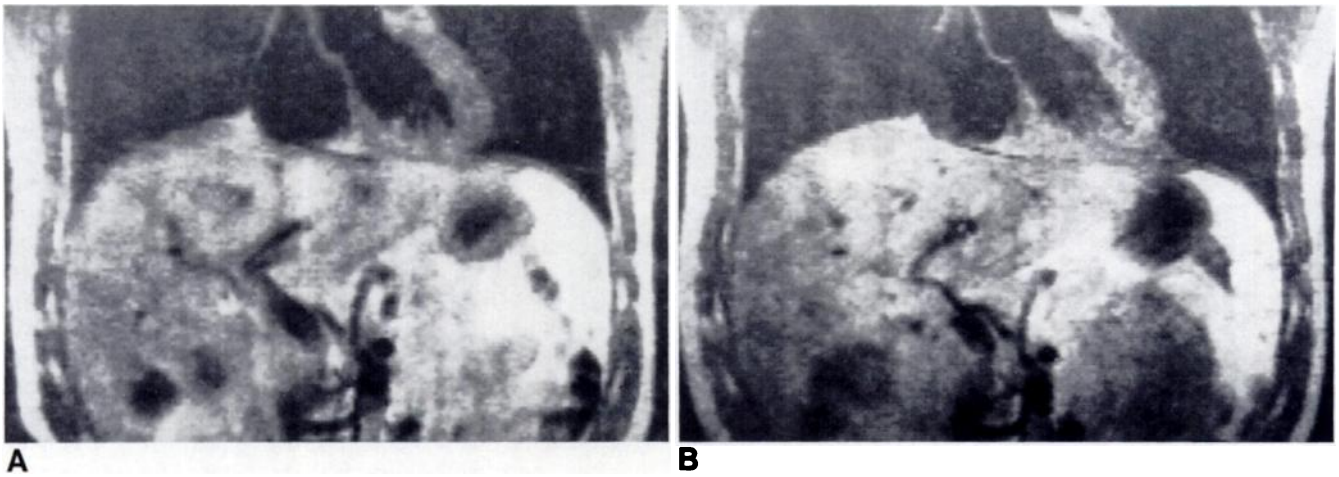

Fig. 9.—Coronal images of upper abdomen and chest. Margin of dome of right hemidiaphragm is slightly better demarcated with combined cardiac and respiratory gating (**B**) than with cardiac gating alone. (**A**).

Effect on Relaxation-Time Measurements

Table 1 summarizes the results of relaxation-time measurements from a uniform tissue-equivalent phantom with and without gating at a simulated respiratory rate of 15/min. There was no significant difference in T1 measured in the nongated study and in the spin-conditioned study. T1 values measured in the non-spin-conditioned study, on the other hand, were substantially different ($p < 0.001$) and erroneously shortened. T2 values with either method of gating were not significantly different from nongated values. T1 measurements obtained from multiple regions of interest in the spleen of a volunteer who was imaged using both types of respiratory gating support the results of the phantom studies. The mean T1 values in gated studies with and without spin-conditioning were 927 msec and 682 msec, respectively.

Table 2 summarizes the results of T1 measurements in multiple splenic and hepatic regions of interest in five volunteers who had nongated and respiratory-gated (spin-conditioned studies). The differences between individuals in the mean T1 value were not statistically significant. The relative standard deviation (SD) of the pooled splenic T1 measure-

TABLE 1: **Relaxation-Time Measurements from Nongated and Gated Images of a Tissue-Equivalent Phantom**

Relaxation Time	Non-gated	Respiratory Gated	
		Spin-Conditioned	Non-Spin-Conditioned
T1 (msec):			
Mean	373	383	312
SD	17	14	11
T2 (msec):			
Mean	59	58	58
SD	1	1	1

Note.—Simulated respiratory rate of 15/min was used for gating.

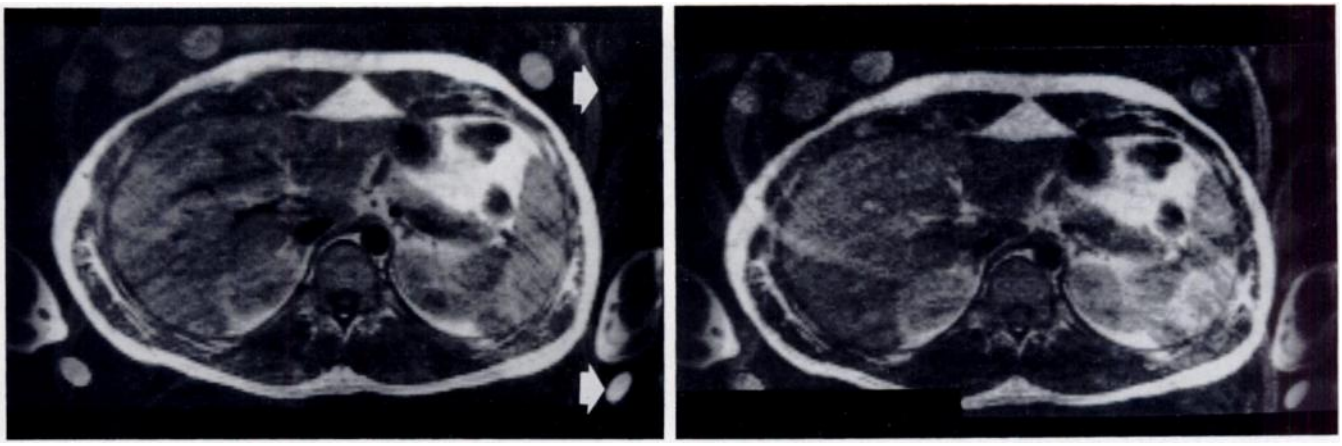

A B

Fig. 10.—Nongated images. **A**, 28 msec TE. **B**, 56 msec TE. Extensive ghost artifact formation due to respiratory motion. Even stationary objects, such as external phantoms, are subject to ghosting (*arrows*), which was eliminated by respiratory gating.

TABLE 2: **Spin-Lattice Relaxation Times of Liver and Spleen for Gated and Nongated Images of Five Volunteers**

Organ: T1 (msec)	Nongated	Respiratory Gated, Spin-Conditioned
Spleen:		
Mean	702	599
SD	300	174
Mean range	466	138
Liver:		
Mean	241	267
SD	105	51
Mean range	145	74

Note.—Mean range values are the average for five volunteers of the difference between the highest and lowest T1 values derived from different regions of interest in the same organ.

ments from the nongated studies was nearly 50% larger than for the gated studies. The relative SD of hepatic T1 measurements was more than twice that of gated studies. Similarly, the mean difference between the highest and lowest parenchymal T1 values for each individual subject was more than three times greater in nongated images of spleen and twice as large in nongated images of the liver. It would seem that respiratory gating will allow calculation of T1 values with lesser individual measurement variations.

Discussion

The motion of abdominal structures during breathing is multidirectional, with components in the longitudinal axis and in the plane of transverse imaging. It is therefore not surprising that these motions can produce complex artifacts in MR images acquired by two-dimensional Fourier transform methods. Before this study, we did not fully appreciate the extent to which superimposed artifacts degrade the diagnostic quality of spin-echo images of the upper abdomen, particularly with short repetition times. Sequences with short TRs are of value because they maximize T1-weighting in SE imaging.

Several different kinds of artifacts are identifiable in our nongated images. The most serious type consists of multiple ghost images displaced from the primary image along the phase encoding axis (fig. 10). We were interested to note that ghosting was not limited to structures in respiratory motion. Figure 10 demonstrates ghosting of stationary phantoms attached to the table posterior to the patient. Respiratory gating was able to abolish most of the artifacts, including ghosting of the stationary phantoms. This finding underscores the complex nature of the process that results in artifact formation.

In summary, our results are in agreement with those of others [8, 9], indicating that respiratory gating leads to substantial improvement in the diagnostic quality of MR images of the upper abdomen. The relative improvement compared with nongated studies was greatest for SE images with short TRs.

The belt device was found to be the best method for obtaining a respiratory signal on the basis of reliability and patient comfort. Other techniques remain to be tried, including impedance plethysmography, which is particularly attractive because it requires only the attachment of chest electrodes and is potentially superior.

The time penalty for respiratory gating is strongly dependent on technique and breathing pattern. The increase in imaging time is 100%–300% with tidal breathing, but this can be reduced to only 30%–50% by simple maneuvers. Such modified breathing patterns would obviously be applicable only to cooperative patients who are not in respiratory distress. A method of providing feedback to the patient indicating when image data were successfully being acquired would be helpful.

Simple triggered respiratory gating without spin-conditioning results in images that have more detail than nongated studies, but which are inferior to spin-conditioned studies. Without spin-conditioning, the presence of occasional long periods of tissue relaxation when sequencing is halted leads to systematic errors in T1 measurements.

Spin-conditioning respiratory gating causes no systematic errors in T1 or T2 values compared with nongated studies. The scatter of in vivo T1 measurements is markedly reduced by respiratory gating, most likely due to the reduction of superimposed artifact.

It is clear that respiratory-gated images are likely to allow depiction of small lesions in the abdomen that would otherwise not be seen due to motion blur. In addition, removal of superimposed artifact leads to an improvement in contrast resolution in a manner analogous to reducing scatter in radiography. Thus, for example, renal cortex and medulla can be more clearly differentiated (figs. 4, 5A, and 5B).

Given the inherent time penalties with respiratory gating, we believe that the best use of limited imaging resources will be in selected cases rather than routinely. The indications will depend on the type of lesion that is being investigated. Usage will also be influenced by whether the patient is capable of simple respiratory maneuvers that can reduce imaging time.

REFERENCES

1. Crooks LE, Ortendahl DA, Kaufman L, et al. Clinical efficiency of nuclear magnetic resonance imaging. *Radiology* **1983**;146:123–128
2. Crooks LE, Arakawa M, Heonninger J, et al. Nuclear magnetic resonance whole-body imager operating at 3.5 kgauss. *Radiology* **1982**;143:169–174
3. Wood M, Henkelman RM. NMR image artifacts from periodic motion (abstr). In: *Proceedings of the Society of Magnetic Resonance in Medicine, Second Annual Meeting, San Francisco*, August **1983**:380
4. Kundel H, Kressel H, Thickman D, Axel L. Motion produces y-direction ghost artifacts in NMR spin-warp imaging (abstr). In: *Proceedings of the Society of Magnetic Resonance in Medicine, Second Annual Meeting, San Francisco*, August **1983**:204
5. Nelson AD, Alfidi RJ, Kopiwoda S, Miraldi F, Clampitt M. Experimental characterization of motion artifact in NMR images (abstr). In: *Proceedings of the Society of Magnetic Resonance in Medicine, Second Annual Meeting, San Francisco*, August **1983**:9
6. Lanzer P, Botvinick EH, Schiller NB, et al. Cardiac imaging using gated nuclear magnetic resonance. *Radiology* **1984**;150:121–127
7. Fletcher BD, Jacobstein MD, Nelson AD, Riemenschneider TA, Alfidi RJ. Gated magnetic resonance imaging of congenital cardiac malformations. *Radiology* **1984**;150:137–140
8. Prato FS, Nicholson RL, King M, et al. Abolition of respiratory movement markedly improved NMR images of the thorax and upper abdomen (abstr). In: *Proceedings of the Society of Magnetic Resonance in Medicine, Second Annual Meeting, San Francisco*, August **1983**:284–285
9. Runge VM, Clanton JA, Partain CL, James AE. Respiratory gating in magnetic resonance imaging at 0.5 tesla. *Radiology* **1984**;151:521–523
10. Ehman RL, Kjos BO, Houston MS, Brasch RC, Brant-Zawadzki M, Higgins CB. Spin echo imaging: a method for correction of systematic errors in calculated T1 and spin density (abstr). In: *Proceedings of the Society of Magnetic Resonance in Medicine, Second Annual Meeting, San Francisco*, August **1983**:284–285
11. Herfkens R, Davis PL, Crooks LE, et al. Nuclear magnetic resonance imaging of the abnormal live rat and correlations with tissue characterizations. *Radiology* **1982**;141:211–218